Title: Rhythmic lipid and gene expression responses to chilling in panicoid grasses

Authors: Sunil K. Kenchanmane Raju[1, *, †] (kenchanmane@gmail.com), Yang Zhang[1,*,‡] (yang.zhang@stjude.org), Samira Mahboub[1,2] (samira.mahboub@unl.edu), Daniel W. Ngu[1] (dngu2@yahoo.com), Yumou Qiu[3] (yumouqiu@iastate.edu), Frank G. Harmon[4] (fharmon@berkeley.edu), James C. Schnable[1,5,#] (schnable@unl.edu), and Rebecca L. Roston[1,2,#] (rroston@unl.edu)

* Contributed equally - Sunil K. Kenchanmane Raju and Yang Zhang
# Corresponding authors - James C. Schnable and Rebecca L. Roston

[1]Center for Plant Science Innovation, University of Nebraska-Lincoln, Lincoln, NE, USA
[2]Department of Biochemistry, University of Nebraska-Lincoln, Lincoln, NE, USA
[3]Department of Statistics, Iowa State University, Ames, IA, USA
[4]Plant Gene Expression Center, USDA-ARS, Albany, CA, USA and Department of Plant and Microbial Biology, University of California, Berkeley, CA, USA.
[5]Department of Agronomy and Horticulture, University of Nebraska-Lincoln, Lincoln, NE, USA

†Present Affiliation: Department of Botany and Plant Sciences, University of California, Riverside, CA, USA
‡Present Affiliation: St. Jude Children's Research Hospital, Computational Biology, Memphis, TN, USA

Corresponding Authors:
James C. Schnable
1901 Vine St.
Lincoln, NE, 68588
402-472-4540
schnable@unl.edu

Rebecca L. Roston
1901 Vine St.
Lincoln, NE, 68588
402-472-2936
rroston@unl.edu

Preprint Servers: bioRxiv

Date of Submission: 01/24/2024

Word count: 7645 (Abstract – Discussion)

HIGHLIGHT

Chilling stress triggers distinct, time-specific lipid and transcriptional responses in cold-tolerant foxtail millet compared to their non-tolerant relatives, elucidating species-specific adaptations, and conserved circadian rhythms across plants.

ABSTRACT

Chilling stress threatens plant growth and development, particularly affecting membrane fluidity and cellular integrity. Understanding plant membrane responses to chilling stress is important for unraveling the molecular mechanisms of stress tolerance. Whereas core transcriptional responses to chilling stress and stress tolerance are conserved across species, the associated changes in membrane lipids appear to be less conserved, as which lipids are affected by chilling stress varies by species. Here, we investigated changes in gene expression and membrane lipids in response to chilling stress during one 24 hour cycle in chilling-tolerant foxtail millet (*Setaria italica*), and chilling-sensitive sorghum (*Sorghum bicolor*), and Urochloa (browntop signal grass, *Urochloa fusca*, lipids only), leveraging their evolutionary relatedness and differing levels of chilling-stress tolerance. We show that most chilling-induced lipid changes are conserved across the three species, while we observed distinct, time-specific responses in chilling-tolerant foxtail millet, indicating the presence of a finely orchestrated adaptive mechanism. We detected rhythmicity in lipid responses to chilling stress in the three grasses, which were also present in Arabidopsis (*Arabidopsis thaliana*), suggesting the conservation of rhythmic patterns across species and highlighting the importance of accounting for time of day. When integrating lipid datasets with gene expression profiles, we identified potential candidate genes that showed corresponding transcriptional changes in response to chilling stress, providing insights into the differences in regulatory mechanisms between chilling-sensitive sorghum and chilling-tolerant foxtail millet.

Key words: Chilling stress, panicoid grasses, lipid abundance, lipid unsaturation, diel rhythms

Abbreviations: thin layer chromatography (TLC), Fragments Per Kilobase of transcript per Million mapped reads (FPKM), differential regulated orthologs (DRO), false discovery rates (FDR), linear mixed model (LMM), monogalactosyldiacylglycerol (MGDG), digalactosyldiacylglycerol (DGDG), phosphatidylcholines (PC), triacylglyceride (TAG),

phosphatidylglycerol (PG)

Introduction:

Climate change has increased the frequency and severity of extreme weather events, threatening future food supply (Ray et al. 2013). Major crop species important for global food security, such as maize (*Zea mays*), sorghum (*Sorghum bicolor*), and rice (Oryza sativa), are sensitive to chilling stress owing to their tropical origin, limiting their geographical distribution and productivity in temperate climates (Lyons 1973; Taylor and Rowley 1971). Chilling stress is major stress experienced by plants during their lifecycle, hindering energy metabolism and growth, most notably by reducing the activity of enzymes associated with photosynthesis and the energy-demanding production of protective proteins and substances (Kaplan and Guy 2004; Hurry et al. 2002). Moreover, plants must endure daily and seasonal temperature fluctuations and unexpected extreme variations (Larran, Pajoro, and Qüesta 2023). Plants have devised various strategies to cope with such environmental challenges.

At the cellular level, low-temperature stress leads to increased membrane rigidity and impaired containment of cytosolic contents, resulting in cell death (Zoldan et al. 2012; Matsuo Uemura et al. 2006). Changes in glycerolipids, major components of cell membranes, include membrane lipid polyunsaturation (Hugly and Somerville 1992; Miquel et al. 1993), changing the ratio of lipid head groups, and removing membrane-destabilizing lipids in response to low temperature (Moellering, Muthan, and Benning 2010; Barnes, Benning, and Roston 2016). The contribution of unsaturated fatty acids to membrane fluidity at different temperatures and their role in protecting the photosynthetic machinery from photoinhibition under chilling stress are well known (Nishida and Murata 1996). However, no consistent changes in membrane lipid abundance during chilling stress have been reported across species. These discrepancies in

changes in lipid compositions or content during stress may be due to differences in the duration and/or intensity of the applied stress, time-of-day effects, and/or genetic and physiological differences across species (Kenchanmane Raju et al. 2018).

Plant responses to these stressful environments can vary greatly at the transcriptional level, although a core set of transcriptional responses is mostly conserved across species (Kenchanmane Raju et al. 2018). Notably, most studies of cold tolerance in the Pooideae grass subfamily of the Poaceae (including wheat [*Triticum aestivum*], barley [*Hordeum vulgare*], and rye *[Secale cereale*]) have revealed chilling adaptive mechanisms that are not shared by closely allied subfamilies within the grasses, such as the Ehrhartoideae (which includes rice). This lack of conservation suggests that different plant lineages have adapted to growth in temperate environments using distinct genetic and physiological mechanisms. Panicoid grasses, comprising many important crops such as maize, sugarcane (Saccharum officinarum), switchgrass (*Panicum virgatum*), sorghum, and foxtail millet (*Setaria italica*), exhibit a range of sensitivities to cold temperatures (Hope and McELROY 1990; Dohleman and Long 2009; Kenchanmane Raju et al. 2018). The repeated acquisition and loss of chilling tolerance within this subfamily (Sandve et al. 2008; Pardo and VanBuren 2021) make it an ideal system to study the conserved and species-specific adaptation strategies for chilling tolerance.

Sorghum, an important crop in the arid and semi-arid regions of the world, originated in the semi-arid tropics of Africa and quickly spread into other parts of the world, including India, China, and the United States (Doggett and Majisu 1968). Due to its tropical origin, sorghum is susceptible to chilling (Burow et al. 2011). While landraces and wild relatives are important gene pools for adaptive traits such as biotic stress resistance and abiotic stress tolerance (Brozynska,

Furtado, and Henry 2016), the limited availability of standing genetic variation and newer cropping environments require the transfer of stress adaptation mechanisms from closely related stress-adapted species. Like sorghum, foxtail millet is also a grain crop domesticated from a panicoid grass. However, foxtail millet was initially domesticated in northeast China from a wild grass, green foxtail (*Setaria viridis*) that grows in temperate climates where low-temperature stress is more common (Yang et al. 2012; G. Zhang et al. 2012; Bennetzen et al. 2012).

Orthologous genes, even within closely related taxa, can show differential regulation of chilling stress responsive gene expression between maize and sorghum, or between maize, sorghum and eastern gamagrass (*Tripsacum dactyloides*) (Y. Zhang et al. 2017; Yan et al. 2019), suggesting that orthology alone is not a reliable predictor of stress-induced gene expression in related species (Meng et al. 2021). It can therefore be challenging to narrow down target genes for chilling-stress tolerance in sorghum and related chilling-sensitive species.

To overcome these challenges, we designed a time-course experiment to account for potential time-of-day variation and tested the relationship between chilling-stress tolerance, changes in membrane glycerolipid contents, and evolutionary relatedness using three panicoid grasses. Browntop signal grass (*Urochloa fusca,* Urochloa hereafter) is a grass closely related to foxtail millet that is less chilling tolerant. Urochloa and sorghum are more distantly related and have similar susceptibility to chilling stress. In this study, we profiled the changes in membrane lipid contents and composition and in transcript levels in these three species using paired time-course measurements of control and chilling-stress conditions. We identified differentially regulated genes increased in chilling-tolerant foxtail millet, including 3-KETOACYL-COA

SYNTHASE 1 (KCS1), known for its effects on chilling stress tolerance. We also showed that correlating lipid abundance changes with gene expression profiles allowed the identification of lipid metabolic genes responding to chilling within a species, such as sorghum's DIGALACTOSYL DIACYLGLYCEROL DEFICIENT 1 (SbDGD1). These genes have potential application in engineering chilling tolerance in sorghum and related chilling-sensitive grasses.

Materials and Methods

Plant growth and chilling treatment

Seeds for the reference genotypes for sorghum (*Sorghum bicolor, BTx623*), maize (*Zea mays*, *B73*), Urochloa (*Urochloa fusca, LBJWC-52*) and foxtail millet (*Setaria italica, Yugu1*) were grown in a Percival growth chamber (E-41L2) with 60% relative humidity, with a 12 h light/12 h dark photoperiod and a target temperature of 29□ during the day and 23□ at night. Chilling stress was applied to 12-day-old seedlings, when collars of two leaves are visible. Immediately at the end of the light period, seedlings were moved to a second growth chamber with identical photopheriod settings and a target temperature of 6□. Each sample represents a pool of above-ground tissue from at least three seedlings. Samples were harvested from the control conditions and chilling stress treated plants at the designated time points after the onset of chilling stress. Arabidopsis of the Columbia ecotype were planted as described (Barnes et al. 2023), and grown under a 16h light/8 h dark photoperiod to enhance the effect of initial chilling in this frost-tolerant species. Chilling stress was applied to 4-week-old rosettes, at the transition to flowering. Immediately at the end of the light period, seedlings were moved to a second growth chamber with equivalent identical settings and a target temperature of 6□

For lipid analysis, whole shoot tissue of seedlings was removed at soil level, excluding the coleoptile of grasses. Samples were harvested at 0 min (immediately before

reducing the chamber temperature to 6□), 10 min, 3 h, 6 h, 12 h, and 24 h. The 10-minute sample was taken 10 after the chamber air temperature reached 6□, approximately 20 minutes past time 0. Whole shoot tissue excluding the coleoptile, was collected at the soil level. Due to a combination of sample loss during processing and outlier analysis, the number of represented biological replicates changed by the lipid species analyzed (always ≥ 3 biological replicates for each growth / treatment trial). The tissue was quickly and gently submerged in 1 mL of ice-cold extraction solvent (2:1:0.1 v/v/v methanol:chloroform:formic acid) in a 2 ml tube and shaken on a bead beater at 4000 inversions per minute in 30-second intervals with intervening ice incubations until the tissue was thoroughly disrupted. Lipid extraction continued following a modified Bligh and Dyer protocol (Mahboub et al. 2021). Following extraction, lipids were concentrated and stored at -80□ under nitrogen. Lipids were separated as described in Wang and Benning (Wang and Benning 2011) with the following modifications. A 10% lipid spot was loaded in the corner of each thin layer chromatography (TLC) plate that did not see solvent which served as a control for total fatty acids and was used to make internal comparisons.

A two-dimensional TLC plate was used for separation. In the first dimension, a mixture of chloroform: methanol: ammonium hydroxide, (130:50:10, v/v/v) was used as solvent and in the second dimension, chloroform: methanol: acetic acid: water (85:12.5:12.5:4, v/v/v/v) was used as a solvent. A separate one dimensional thin-layer chromatogram was used to separate non-polar triacylglcyerol, with petroleum ether:diethyl ether:acetic acid (80:20:1, v/v/v) as solvent. Lipids were identified by retention time compared to standards purchased from Avanti Polar Lipids. Remaining analysis was precisely done as described in Barnes et al 2016 (Barnes, Benning, and Roston 2016)

The statistical analysis of lipid data involved several steps. Outliers were assessed at two levels. Firstly, for fatty acid abundance, a robust regression of outlier removal (ROUT) analysis was performed at a 10% threshold using GraphPad v9.5.0 to eliminate any misidentified peaks or anomalies. Any outliers detected at this step were removed from further analysis. Second, the relative mole percentages of each lipid were calculated and normalized to the total fatty acids present. The resulting mole percentages were then screened for outliers using one interquartile distance from the median for each lipid class for each genotype at each temperature. Asterisks denote statistical significance ($p \leq 0.05$), determined by fitting a mixed model, with Tukey's correction for multiple tests. Due to a combination of manual error causing sample loss during processing and outlier analysis, the exact number of represented biological replicates changed by the lipid species analyzed, always between 3 and 8 biological replicates for each split among at least two separate growth trials.

The double bond index (DBI) was calculated using the formula: (X:1)×1+(X:2)×2+(X:3)×3)/100, where X represents the relative mole % of 16:n and 18:n fatty acids, and n denotes one, two, or three double bonds. Multiple comparisons were adjusted using Tukey's multiple comparisons test when comparing between genotypes.

Measurement of CO_2 assimilation rates

Seedlings were grown and stress treated as above, with the modification that small plastic caps were placed over sorghum, foxtail millet, and Urochloa seedlings to prevent them from becoming too tall to fit into the LI-COR measurement chamber. After 0, 1, or 8 days of chilling treatment, seedlings were allowed to recover in the greenhouse overnight under control

conditions and CO_2 assimilation rates were measured the next morning using the LI-6400 portable photosystem unit under the following conditions: PAR 200 µmol mol−1, CO_2 at 400 µmol mol−1 with flow at 400 µmol mol−1 and humidity at greenhouse conditions. Whole seedlings readings were measured for sorghum, foxtail millet, and Urochloa after covering the pots with clay and using the LI-COR's Arabidopsis chamber. Readings for maize were measured using the leaf clamp attachment which was always placed on the second leaf at a position 3 cm above the ligule. Leaf area was measured using the LI-3100C area meter.

RNA isolation and RNA-seq analysis

Total RNA was isolated from paired samples collected at 30 min, 1 h, 3 h, 6 h, 16 h, and 24 h after the onset of chilling. Library construction was performed following the protocol described by Zhang et al. 2017 (Y. Zhang et al. 2017). Sequencing was conducted at the Illumina Sequencing Genomics Resources Core Facility at Weill Cornell Medical College. Raw sequencing data are available through the NCBI (http://www.ncbi.nlm.nih.gov/bioproject) under accession number SRA: SRP090583 and BioProject: PRJNA344653. Summary statistics for all the libraries are provided in Table S1. Adapters were removed from the raw sequence reads using *cutadapt* v*1.6*. RNA-seq reads were mapped to genome assemblies downloaded from Phytozome (v13): v3.1 (sorghum) and v2.2 (foxtail millet). RNA-seq reads from each species were aligned using GSNAP (Wu et al. 2016) and Fragments Per Kilobase of transcript per Million mapped reads (FPKM) values were obtained using cufflinks v2.2.1 (Trapnell et al. 2010).

Syntenic orthologs in sorghum and foxtail millet

A final set of 9778 syntenic orthologous gene pairs between sorghum and foxtail millet was calculated from the previously published list of syntenic orthologs(Schnable, Zang, and Ngu

2016) after filtering for standard deviation < 0.4 and r-square > 0.1 of the FPKM values (**Table S5**). Clustering was performed using 'correlation' from R packages 'fpc' ("Fpc: Flexible Procedures for Clustering" n.d., "'Finding Groups in Data': Cluster Analysis Extended Rousseeuw et Al. [R Package Cluster Version 2.1.4]" 2022). To observe treatment effects, the ratio between treatment FPKM and control FPKM was determined for the time course. A permutation test was performed by keeping the sorghum gene constant and randomly assigning a different foxtail millet gene 100 times to determine the appropriate r2, standard deviation, and number of clusters. Syntenic orthologs found within the same clusters were considered co-expressed (CEO), while syntenic orthologs found in different clusters were considered as differentially expressed orthologs (DEO)

Identification of differentially regulated orthologs

The FPKM values were measured from three biological replicates each for sorghum and foxtail millet under control and cold treatment at six time points (30 min, 1 h, 3 h, 6 h, 16 h, and 24 h). Similar to the cluster analysis, the treatment over control (T/C) FPKM ratios at each time point for sorghum and foxtail millet were calculated and treated as a response. A linear mixed model (LMM) was used to model the T/C ratios as a relationship between the species identity and sampling time under chilling stress on the same set of syntenic orthologous gene pairs used in the cluster analysis. Let yijkl denote the T/C ratio of the ith gene from the kth species and the lth biological replication at the jth time point, where j = 1-6 to represent the six time points, k = 1, or 2 to represent the two species: sorghum and foxtail millet, and l = 1, 2, or 3 to represent the three biological replicates. There was a total of six biological replicates in the study, three from sorghum and three from foxtail millet. We modeled the biological replication as a random effect. For the ith gene, conditioned on this random replication effect, the response yijkl is normally

distributed with mean μijkl and variance σ 2 i. The expected T/C ratio μijkl was linearly related to the species, time and their interactions as μijkl = νi + αij + βik + γijk + ηikl for ηikl ∼ N(0, θ2 i), (1) where νi is the intercept; αij and βik stand for the main effect of time and species for the ith gene respectively; γijk is the interaction between time and species, denoting different patterns of expression between the two species over time; and ηikl is the random effect for the biological replicates, which is assumed to be normally distributed with mean 0 and variance θ 2 i . Note that the interaction effect γijk in the model (1) stands for the difference of the T/C ratios over time between sorghum and foxtail millet. The non-zero interaction effect represents different patterns of T/C ratios changing over time between the two species, while the zero γijk indicates a similar trend of the responses of the two species. Those genes with nonzero interaction effect are defined as differential regulated orthologs (DRO) and the ones with zero interaction effect are called comparable regulated orthologs (CRO). In order to identify the DROs, we considered the hypotheses Hi,0: γijk = 0 for all j, k vs. Hi,a : γijk 6= 0 for some j, k (2) for each gene. Estimation of γijk and its associated standard error were obtained by the *'lmer'* function in the R package *lme4*. Wald test statistic was conducted for the hypothesis (2), and the associated p-value for each gene was calculated. Benjamini and Hocheberg multiple test correction was applied to control for false discovery rates (FDR) > 0.001. Those pairs with FDR < 0.001 were considered as DRO, and those with FDR > 0.01 were considered as CROs.

Lipid genes in sorghum and foxtail millet.

A manually curated list of Arabidopsis genes known to be involved in lipid pathways was first created using the Aralip database (http://aralip.plantbiology.msu.edu/pathways/pathways). The sorghum and foxtail millet genes were then matched to the Arabidopsis lipid genes using the published best Arabidopsis hits for the sorghum and foxtail millet genome on Phytozome (v13).

Each sorghum and foxtail millet hit was matched with their respective syntenic ortholog in the other species, creating a list of syntenic orthologous pairs of lipid genes in sorghum and foxtail millet (Table S9).

Gene expression and lipid heatmaps

FPKM values and lipid abundance and unsaturation were normalized by linear transformation such that the minimum value within the time series turned into a zero and maximum values are turned to one. All other values get transformed into decimals between 0 and 1. Heatmaps were generated using heatmap2 function in R.

Identification of rhythmicity in lipid abundance and expression of lipid related genes.

Rhythms in lipid abundance were identified with the 'circa_single' method in CircaCompare (package version 0.1.1) in R (version 4.3.0) with default settings (Parsons et al. 2020). Differences in lipid abundance waveforms were detected with the 'circacompare' method in the same package. FPKM values representing expression at 3-hour intervals over 72-hours for the 356 lipid-metabolism-associated genes that were syntenic between sorghum and foxtail millet were derived from previously published transcriptomes of comparably staged third-leaf-stage seedlings from sorghum, foxtail millet, and maize (Lai et al. 2020). Genes in the 356 metabolism-associated data set exhibiting differential rhythmicity between temperature treatments (i.e., cold treatment vs. no treatment) or genotypes (sorghum vs. foxtail millet) were identified with the R package *LimoRhyde (Singer and Hughey 2019)* in Bioconductor (Gentleman et al. 2004). *LimoRhyde* reports Benjamini and Hochberg q-values(Benjamini and Hochberg 1995) of the rhythmicity of gene and diifferential rhythmicity for genes shared

between the two data sets. Statistical significance for either rhythmicity or differential rhythmicity was set at a q-value of ≤ 0.05. Foxtail millet genes were keyed to their sorghum synteologs for *LimoRhyde* identification of differential rhythmicity between sorghum and foxtail millet genes.

Results:

Foxtail millet is chilling tolerant compared to other panicoid grasses.

Chilling stress causes structural transitions in biological membranes of cold-susceptible plants. These membrane changes cause respiration abnormalities and photosynthetic CO_2 and O_2 exchange rates(Lyons 1973; Larcher 1995). Lower photosynthesis for prolonged periods, continuing for hours or days, is an essential identifier of chilling susceptibility(Larcher 1995). Here, we used, CO_2 assimilation rates to quantitatively assess differences in chilling tolerance among closely related panicoid grasses (**Figure 1A**)(Y. Zhang et al. 2017). Accordingly, we measured 12-day-old seedlings grown under control conditions (29□ during the day and 23□ at night) and after exposure to chilling treatment (6□) in growth chambers for one or eight days. After eight days of chilling stress, sorghum, Urochloa, and maize showed lower values for CO_2 assimilation compared to the control time point, indicating impaired photosynthetic activity. In fact, sorghum and Urochloa seedlings had dead leaves, which was reflected in the negative CO_2 assimilation values (**Figure 1B**). Foxtail millet showed moderate impairment in its photosynthetic rate as its CO_2 assimilation measurements remained at about 55% of control levels even after eight days of stress, indicating higher tolerance to chilling (**Figure 1B**) consistent with its native range and center of domestication in Northern China(H. Lu et al. 2009; G. Zhang et al. 2012). Based on these photosynthetic measurements, we classified the four panicoid species into two categories: chilling-susceptible - sorghum, Urochloa, and maize, and chilling-tolerant - foxtail millet. Prolonged stress clearly differentiated tolerance levels in foxtail millet. Following two weeks of chilling stress at 6□ and two days of return to normal growing

temperatures, Urochloa and sorghum seedlings were dead while foxtail millet seedlings looked healthier with fewer necrotic leaves (**Figure 1C**).

Foxtail millet membranes have distinct responses to chilling stress.

Many cellular membrane systems are damaged in response to chilling (Nishida and Murata 1996; Lyons 1973), and changes in membrane lipid compositions are required to achieve chilling tolerance (M. Uemura, Joseph, and Steponkus 1995; Zoldan et al. 2012). We profiled membrane lipids from sorghum, Urochloa, and foxtail millet seedlings grown under control and chilling-stress conditions. We hypothesized that patterns unique to foxtail millet and not in both sorghum and Urochloa potentially stem from the difference in chilling tolerance among the species. Likewise, patterns in foxtail millet that are shared by Urochloa but not sorghum are likely to reflect their closer evolutionary relationship. We collected samples for lipid profiling at 10 min, 3 h, 6 h, 12 h, 16 h, and 24 h following the onset of chilling stress. Of the 11 lipids measured (**Table S1**), nine lipids exhibited 24-hour rhythmic accumulation (rhythmic hereafter) in at least one species (**Table S2**) (Singer and Hughey 2019). In foxtail millet, all three major membrane lipids, monogalactosyldiacylglycerol (MGDG, LimoRhyde, q-value = 0.07), digalactosyldiacylglycerol (DGDG, LimoRhyde q-value =0.04), and phosphatidylcholines (PC, LimoRhyde q-value =0.03) were found to be rhythmic (Figure 2, Table S2). PC was rhythmic in all three species, while triacylglyceride (TAG) and phosphatidylglycerol (PG) were rhythmic in sorghum and Urochloa. Major lipids such as DGDG and PC were rhythmic in foxtail millet and Urochloa (**Figure 2A**), suggesting a strong influence of genetic relatedness on major lipid abundance patterns. However, a foxtail millet-specific increase in MGDG abundance was observed at 24 hr post chilling stress compared to sorghum and Urochloa (p-value = 0.003 and p-value = 0.004, respectively) (**Figure 2A**). Further, we tested the difference in rhythmicity in PC

and DGDG between species using CircaCompare analysis (Parsons et al. 2020). The time at which the metabolites (response variable) reach peak abundance (phase) is significantly different for PC in all three species (**Table S3**). Mesor, a rhythm-adjusted mean, is significantly different in foxtail millet compared to sorghum (p-value = 0.001) and Urochloa (p-value =0.006). We also examined the variation in rhythmicity of lipid saturation levels among species. In foxtail millet, DGDG, MGDG, PC, and total saturation exhibited significant rhythmicity, whereas in Urochloa only PC and total saturation showed significant rhythmicity. In sorghum, only total lipid saturation displayed significant rhythmicity (**Table S3**). These results show that rhythmic lipids across species differ in their rhythmicity or peak and mesor values suggesting species-specific control of rhythmicity in lipid content and composition.

Similar headgroup and fatty acid tail sizes in lipids like PC and DGDG favor strong interactions that stiffen membranes during cold stress, while smaller headgroups like MGDG's promote fluidity at lower temperatures (**Figure 2C**). We initially expected a dip in PC and DGDG levels alongside corresponding climbs in PE and MGDG during chilling but observed no such trend within the first 24 hours for any species (**Figure 2A, Figure S1**). This prompted us to shift our focus to fatty acid unsaturation, as it affects the head-to-tail size ratio and influences membrane fluidity. Further, low temperature-induced increases in fatty acid polyunsaturation of membrane lipids are associated with greater membrane fluidity and increased chilling tolerance (Quinn, Joo, and Vigh 1989; Miquel et al. 1993). We detected significant differences in DGDG unsaturation levels in foxtail millet compared to Urochloa following 3 h of chilling stress and relative to Urochloa and sorghum at 6 h of chilling stress, indicating a foxtail millet-specific early stress response (**Figure 2B, Table S4**). We observed similar species-specific differences in lipid unsaturation levels for minor lipids such as phosphatidylethanolamine (PE), phosphatidylinositol (PI), phosphatidylglycerol (PG), phosphatidylserine (PS), and sulfoquinovosyldiacylglycerol

(SQDG) (**Figure S1**). The total lipid unsaturation index remained high for sorghum throughout the time course, while foxtail millet and Urochloa were characterized by lower unsaturation near the end of the time course (**Figure 2D, Table S4**). Thus, neither the bulk changes in lipid head groups nor unsaturation in these species can explain the increased low-temperature tolerance of foxtail millet in the first 24 hours of chilling.

Transcriptional changes in lipid metabolism genes are associated with lipid abundance change.

In previous work, we have shown that lipid pathway genes were differentially regulated in temperate-adapted *Tripsacum dactyloides* compared to maize and sorghum in response to chilling stress and were enriched among genes experiencing rapid rates of protein sequence evolution in *T. dactyloides* (Yan et al. 2019). To examine whether transcriptional changes in lipid metabolism genes match the observed patterns of lipid changes between chilling-tolerant foxtail millet and chilling-sensitive sorghum, we collected samples from sorghum and foxtail millet for transcriptome sequencing (RNA-seq) at 30 min, 1 h, 3 h, 6 h, 16 h, and 24 h after the onset of chilling stress, as well as from paired control samples not exposed to chilling stress, collected at the same time points. We employed a conventional correlation co-expression clustering method and a linear mixed model (LMM) based method to understand the differences and commonalities in how sorghum and foxtail millet respond to chilling stress at the transcriptional level (see Methods).

We used a set of 16,796 syntenic orthologous gene pairs conserved between sorghum and foxtail millet (25). Of these, 9,778 gene pairs passed an expression data quality filter of standard

deviation < 0.4 and r-square > 0.1 (**Table S5**, see Methods). Of this filtered set, 2,233 gene pairs (**Table S6**) exhibited a significant species * treatment interaction effect (multiple testing corrected false discovery rate [FDR] < 0.001(Benjamini and Hochberg 1995), indicating differences in the chilling stress-induced transcriptional response of orthologous genes between the two species. In parallel, we applied conventional correlation clustering analysis to identify co-expressed syntenic orthologous gene pairs in sorghum and foxtail millet. We used the ratio of expression values between treatment and control conditions for clustering analysis. Using a permutation test, we defined 16 clusters (see methods; (**Figure S2; Table S7**) and identified 2,245 syntenic orthologous genes in different clusters as being co-expressed orthologs. We classified the remaining 7,533 syntenic orthologs as non-co-expressed orthologs and referred to them as correlation cluster - differentially regulated orthologs (CC-DROs, Table S8). Clusters 2, 4, 6, and 14 had more sorghum genes, while clusters 1, 3, 5, 7, 8, 9, 10, 11, and 13 have higher proportions of foxtail millet genes. Clusters 12, 15, and 16 had a similar number of genes from sorghum and foxtail millet (**Table S7**). Clusters 1, 3, 6, and 7 contained genes up-regulated at 6 hr into stress, indicating a possible role in early chilling-stress response. We illustrate the divergence in transcriptional responses to chilling between syntenic gene pairs in a Circos plot, in which lines that cross over between groupings in the center of the chart represent genes that are syntenic orthologs and have distinct patterns of gene expression between foxtail millet and sorghum (**Figure S2**).

We then identified high-confidence differentially regulated orthologs (HC-DROs) by taking the overlap of CC-DROs identified by the clustering method and the DROs identified with LMM (**Table S9**). We determined that 1,708 syntenic orthologous gene pairs overlap in the two sets, which we further used for gene ontology term enrichment (GO) analysis. GO analysis of these 1,708 HC-DRO pairs revealed enrichment for two GO categories: ‘stress response’ and

433 'macromolecule metabolic process'. In validation of our focus on lipids, we observed an
434 enrichment for the GO metabolic process category, 'lipid metabolic process' (GO:0006629, p-
435 value=0.003, **Table S10**).

436

437 We then defined a set of *a priori* candidates from the most likely set of Arabidopsis (*Arabidopsis*
438 *thaliana)* lipid genes corresponding to fatty acid and glycerolipid metabolism from the AraLipid
439 database (http://aralip.plantbiology.msu.edu/pathways/pathways), and a corresponding set of
440 356 sorghum-foxtail millet gene pairs homologous to these Arabidopsis genes with syntenic
441 orthologs in both sorghum and foxtail millet. (**Table S11**). The overall gene expression patterns
442 of these 356 gene pairs revealed that lipid-related genes are mostly up-regulated under chilling
443 treatment in chilling-tolerant foxtail millet, but not in sorghum. Of the 356 lipid-related gene pairs,
444 34 showed differential responses to chilling stress between sorghum and foxtail millet, with
445 pronounced up-regulation of lipid-related gene expression in foxtail millet exposed to chilling
446 stress (**Figure 3, Table S12**). One example of such a differentially regulated ortholog in
447 sorghum and foxtail millet is provided by *3-KETOACYL-COA SYNTHASE 1 (KCS1)*, encoding
448 an enzyme in the fatty acid elongation pathway for wax biosynthesis and involved in chilling
449 tolerance in Arabidopsis(Chen et al. 2020). The sorghum ortholog of *KCS1*, Sobic.001G438100,
450 was down-regulated throughout the chilling-stress time course. However, the *KCS1* ortholog in
451 the chilling-tolerant foxtail millet, Seita.9G470700, was upregulated at later time points (**Figure**
452 **3**), suggesting that the differential regulation of *KCS1* ortholog expression between sorghum
453 and foxtail millet may be leading to the differences in chilling tolerance between the two species.

454

455 **Gene expression correlation with lipid buildup and breakdown**

We asked whether changes in the expression of genes in lipid pathways in foxtail millet and sorghum were consistent with changes in lipid abundance and saturation. To this end, we combined time-course lipid and gene expression profiles to understand how differential gene expression in these two species affects lipid abundance and saturation under chilling stress, using only shared time points between the two datasets. A diagram of the glycerolipid biosynthesis pathway is shown in **Figure 4A**. Looking at the sorghum ortholog of Arabidopsis *DIGALACTOSYL DIACYLGLYCEROL DEFICIENT 1 (DGD1)*, Sobic.006G075100, its expression profile had a positive correlation with DGDG accumulation during chilling (Pearsons's correlation coefficient (PCC r = 0.85, p-value = 0.03). However, the expression of the *DGD1* ortholog in foxtail millet was not correlated with DGDG accumulation (**Figure 4B**). Similarly, the expression of *NON-SPECIFIC PHOSPHOLIPASE C1 (NPC1)* orthologs in sorghum and foxtail millet was positively correlated with PE accumulation during chilling (PCC r = 0.79, p-value = 0.06; PCC r =0.84, p-value = 0.03, respectively). However, the expression of *NPC2, NPC6,* and *PHOSPHOLIPID N METHYLTRANSFERASE* (*PLMT)* was also positively correlated with PE accumulation in sorghum but not in foxtail millet (**Figure 4C**). Notably, we detected correlations between gene expression and lipid contents for lipids with species-specific changes in lipid abundance, such as MGDG and DGDG, as shown in **Figure 2** and **Figure 4B**.

The accumulation of triacylglycerols (TAGs) in plants arises from multiple sources (Xu and Shanklin 2016; Du and Benning 2016) and TAGs are important for low-temperature tolerance (Klińska-Bąchor et al. 2023; J. Lu et al. 2020; Arisz et al. 2018). Correlating gene expression patterns with TAG abundance was expected to shed light on the potential source of TAG during the chilling response. The expression levels of the foxtail millet ortholog to Arabidopsis *LIPID PHOSPHATE PHOSPHATASE 2 (LPP2)*, Seita.4G217800, showed a significant and positive correlation with lipid abundance in TAG accumulation during chilling stress response in foxtail

millet (PCC r = 0.86, p-value = 0.003). By contrast, the expression levels of the sorghum ortholog to LPP2, Sobic.010G190300, showed no significant correlation with TAG accumulation (**Table S13**). This finding suggests that, at least in foxtail millet, phospholipids are the primary source of chilling-stress-induced TAG accumulation. A list of specific orthologs in foxtail millet and sorghum whose expression levels were significantly correlated with the buildup and breakdown of each lipid species is provided in **Tables S13 and S14**.

Conservation of chilling-induced changes in lipid composition and rhythmicity in Arabidopsis

Previous reports of lipid diel rhythmicity, or rhythmicity on a 24-hour cycle, described changes of specific lipids under normal growing conditions in Arabidopsis (Scheu et al. 2012, Nakamura et al. 2014). To test if differences in rhythmicity were observable between normal and chilling conditions, we quantified representative lipids from Arabidopsis seedlings across a time-course with paired control samples and chilling-stress samples collected immediately before chilling stress (0 h), and after 2 h, 6 h, 10 h, 14 h, 18 h, 22 h, and 26 h of stress. DGDG levels remained constant during normal conditions or chilling stress, whereas MGDG levels were slightly higher upon chilling stress compared to control conditions, reaching statistical significance at 22 h and 26 h into stress (**Figure 5A**). This increase in MGDG levels at the late time points was similar to the significant increase in MGDG after 24 h of exposure to stress in chilling-tolerant foxtail millet compared to chilling-susceptible sorghum and Urochloa (**Figure 2**). PC levels increased and remained higher across the entire time course (**Figure 5A, Table S15**). However, PC saturation under chilling stress conditions was only distinguishable from control samples at a few time points (**Figure 5B, C**). We detected significant rhythmicity in MGDG levels in control conditions (Table S16, rhythmic p-value = 0.005) using the ‘circa_single’ method in CircaCompare analysis (Parsons et al. 2020), and the pattern differed by the end of the 24 hours sufficiently to decrease the rhythmicity prediction below significance. Similar rhythmicity changes were observed for

DGDG and PC saturation levels (**Figure 5B**). CircaCompare analysis supported the significance of DGDG saturation rhythmicity during chilling (**Table S16**, rhythmic p-value = 0.017), but not under control conditions, and PC saturation rhythmicity during control (**Table S16**, rhythmic p-value = 0.013), but not during chilling conditions. Interestingly, the amplitudes of major lipids – MGDG, DGDG, and PC were much lower in Arabidopsis compared to the three grasses. These results suggest the conservation of chilling tolerance-induced changes in lipid content and composition and rhythmic patterns of lipids across grasses and Arabidopsis despite 150 million years of divergence between monocots and eudicots (Brendel, Kurtz, and Walbot 2002).

Lipid-related genes exhibit expression rhythmicity.

The conservation of chilling-induced lipid changes implied that chilling tolerance may have evolved in response to daily rhythms in temperature, and then adapted to seasonal variation (Fig. 5D). To determine which sorghum and foxtail millet lipid-related genes exhibit 24-hour rhythms, we examined the patterns of 356 sorghum-foxtail millet lipid-related gene pairs in a previously published 72 h RNA-seq time-course (Lai et al. 2020). We identified 224 sorghum and 189 foxtail millet genes in this set as being rhythmically expressed. Of these, 145 pairs were rhythmic in both sorghum and foxtail millet. We then used the *LimoRhyde* package(Singer and Hughey 2019) to identify those genes with rhythmic expression under control conditions in our data sets. This analysis indicated that 131 sorghum and 204 foxtail millet lipid-related genes had rhythmic expression patterns under control conditions (**Table S17**). Further, we employed *LimoRhyde* to test for differences in rhythmic expression, or differential rhythmicity (DR), for each gene between the control and chilling treatments in sorghum and foxtail millet. We identified 142 foxtail millet lipid-related genes and 101 sorghum lipid-related genes displaying differential rhythmicity between the control and chilling treatments (**Table S17**). Among the 58 lipid-related gene pairs that showed DR between control and chilling stress in both sorghum and foxtail millet, 36 showed rhythmic expression under control conditions in both species (**Figure**

6A). These lipid-related gene pairs are rhythmic genes that change their rhythmicity patterns under chilling treatment and likely represent shared targets in sorghum and foxtail millet for chilling stress-induced alterations in expression.

An example of such a lipid-related gene whose rhythmic expression under control conditions is altered during chilling stress in both sorghum and foxtail millet was *DGD1* (**Figure 6B, C**). Sorghum and foxtail millet *DGD1* showed similar rhythmic patterns of expression under control conditions. However, their rhythm and magnitude of expression change significantly during chilling stress in both species. Of note, *DGD1* was identified as a differentially regulated ortholog in **Figure 3**. In addition, *SbDGD1* expression during chilling stress was positively correlated with DGDG abundance in sorghum. The foxtail millet *DGD1* ortholog did not show such a correlation, suggesting species-specific changes in their response to chilling stress. These results indicate that differences in the diel regulation of lipid-related genes in sorghum and foxtail millet may lead to differential responses to chilling stress.

Discussion:

Panicoid grasses represent an interesting clade with repeated gain or loss of chilling tolerance, reflecting parallel adaptation strategies in different lineages within the clade. Using representative chilling-susceptible sorghum and chilling-tolerant foxtail millet allowed us to identify changes to transcript and lipid levels that are likely to be functionally linked to variation in chilling tolerance between the related species. We included Urochloa, a chilling-sensitive panicoid grass that is more closely related to foxtail millet, as a control for the large evolutionary divergence between foxtail millet and sorghum.

Here, we assembled time course datasets for transcript levels and lipid metabolic profiling in three panicoid grasses with different genetic relatedness and tolerance to chilling stress to understand whether and how changes in the composition of membrane lipids and

555 corresponding changes in gene expression contribute to chilling tolerance in foxtail millet. Most
556 changes in lipid content and composition were consistent across the three species **(Figure 2A,**
557 **B, D**)**,** likely representing shared responses to chilling stress due to their genetic relatedness.
558 Urochloa appears to behave more like foxtail millet than it does like chilling-susceptible
559 sorghum, likely an effect of its short evolutionary distance compared to foxtail millet. By
560 comparing sorghum to Urochloa, we were able to tease out a small subset of lipid metabolic
561 changes that are unique to foxtail millet, the most chilling tolerant panicoid grass tested in this
562 study (**Figure 2**). These results also indicate that lipid unsaturation is unlikely to be the source
563 of chilling tolerance in foxtail millet, as it is similarly adjusted in all three species during the first
564 24 hours of chilling (**Figure 2B, S2**).

565 There is little consensus in reports of changes in lipid content and composition in response to
566 cold stress across land plants (Kenchanmane Raju et al. 2018). These discrepancies in lipid-
567 related changes may reflect inherent genetic and physiological differences in how individual
568 species respond to chilling stress; alternatively, they may stem from varying experimental
569 designs and variation due to sampling time. Evidence is fast emerging for the role of circadian
570 clock regulation in coordinating dynamic plant responses to daily and seasonal environmental
571 fluctuations (Panter et al. 2019; Espinoza et al. 2010). However, daily rhythms in lipid
572 metabolism had not previously been reported for important clades of crops like panicoid grasses
573 under chilling conditions. Notably, rhythmic changes in lipid composition and gene expression
574 during chilling stress are not similar across species, suggesting that a general strategy is not to
575 stop or slow down the circadian clock during stress, rather plants may have developed species-
576 specific strategies to overcome these challenges. Our time-series dataset of changes affecting
577 lipids during chilling stress in three grasses allowed us to uncover rhythmic patterns of lipid
578 abundance and unsaturation. Moreover, our lipid dataset reveals chilling-tolerance-related
579 changes in lipid abundance and unsaturation at specific time points, potentially explaining part

of the difficulty in extracting conserved patterns for lipids across species in previous reports involving one or a few time points. We also detected rhythmicity in the expression of lipid metabolic genes in both sorghum and foxtail millet. The rhythmic nature of changes in lipids and specific changes during chilling stress were similar between grasses and Arabidopsis, in contrast to other published studies that show differences. These findings highlight the importance of time-series datasets to account for diel cycles in uncovering conserved features of chilling-stress responses across large phylogenetic distances.

The diel variation in lipid abundance observed in Arabidopsis (**Figure 5A**) was roughly half as intense as that observed in the panicoid grasses (**Figure 2A**). This disparity raises the question: why do grasses exhibit such pronounced fluctuations in lipidome composition relative to Arabidopsis? While previous studies in maize, a related panicoid grass, highlight a rhythmic accumulation of lipids and lipid precursors (Li et al. 2020), a potential explanation for the stronger amplitudes in grasses may lie in their C4 photosynthetic architecture. Long et al. (1999) demonstrated higher peak photosynthetic activity in C4 species, and photosynthate can theoretically be directly converted into lipids (Clark and Schwender 2022). Notably, engineered sorghum strains can produce substantial amounts of lipid (Vanhercke et al. 2019). This potentially higher lipid influx in grasses could explain the more pronounced -diel oscillations observed. Additionally, our inability to detect consistent rhythmicity in all major lipids of Arabidopsis may be linked to its overall lower amplitude. However, a definitive understanding of the species-specific variation in lipidome dynamics requires further comparative studies encompassing both transcriptomes and lipidomes, preferably across diverse genotypes and chilling stress conditions with many time points.

One of our most intriguing observations was the diel variation in fatty acid double bond content, observed in both, panicoid grasses and Arabidopsis (**Figure 2D, 5C, Tables S3,S4, S15, S16**). Manipulating desaturase activity to increase unsaturation is a proven strategy for boosting low-

605 temperature tolerance in various plant species, including grasses and Arabidopsis (Wang 2019,
606 Wang 2021, Shi 2018). Similarly, loss of desaturase activity reduces plant low-temperature
607 tolerance (Kunst 1989, Hugly 1992, Miquel 1993, Chen 2013). However, the relationship
608 between fatty acid unsaturation and low temperature is more nuanced than this implies, as
609 analysis of ten published low-temperature treatments revealed a decrease in the double bond
610 index with dropping temperatures (Kenchanmane Raju et al. 2018). In our hands, foxtail millet
611 and Urochloa exhibited a transient rise in total lipid double bond index within the first 10 minutes
612 of chilling exposure, potentially reflecting an adaptation to initial membrane stiffening (**Figure**
613 **2D**, **Figure S4**, **Table S4 S15**). However, this trend did not persist throughout the 24-hour
614 chilling period for any species tested (**Figure 2D, Figure 5C, Table S4, S15**), suggesting that
615 other mechanisms, such as phytosterols or membrane protein interactions, play a role in
616 maintaining membrane fluidity alongside unsaturation during the first 24 hours of chilling.

617 Previous studies in Arabidopsis have documented diel variations in lipid saturation under normal
618 growth conditions (Ekman et al. 2007, Maatta et al. 2012, Nakamura et al. 2014), which has
619 been attributed to light-dependent fatty acid synthesis (Kim et al. 2023, Browse et al. 1981).
620 Congruently, our analysis revealed diel variation in total fatty acid saturation across all three
621 grass species (**Figure 2B, Tables S3, S4**), suggesting a similar underlying biological
622 mechanism. While previous research in Arabidopsis focused on highly unsaturated
623 phosphatidylcholine (PC) molecules peaking in the dark, (Ekman et al. 2007, Maatta et al. 2012,
624 Nakamura et al. 2014) our study did not analyze specific PC molecules. However, we observed
625 rhythmicity in PC saturation across foxtail millet, Urochloa, and Arabidopsis, with overall
626 saturation levels declining in the dark (**Figures 2B, 5B, and Tables S3, S4, Table S15, S16**). In
627 contrast, sorghum did not exhibit similar PC saturation rhythmicity, indicating species-specific
628 differences. Furthermore, species-specific variations in saturation rhythmicity were also
629 observed in MGDG and DGDG among the grass species (**Tables S3, S4**).

Combined lipidomic and transcriptomic analysis has been used to unravel transcriptional regulation of lipid metabolism during chilling-stress responses in maize (Gu et al. 2017). Our results show species-specific differences in transcriptional correlation with lipid metabolic changes, suggesting complex regulation of metabolic perturbations involved in plants' response to environmental challenges. We propose that this approach with chilling-susceptible and chilling-tolerant species can empower the identification of specific genes whose transcript levels are correlated with changes in lipid metabolites, in response to chilling stress. However, our experimental design may miss non-syntenic genes that may have acquired novel chilling-induced changes in their expression. We identified species-specific differences in the extent of correlation between lipid related gene expression and changes in lipid abundance changes, potentially informing the flux of fatty acids. For example, we discovered that the expression of the foxtail millet *LPP2* is tightly correlated with TAG abundance. LPP2 generates DAG from phospholipids in the ER, DAG is a precursor to TAG (**Figure 4A**), implying that that phospholipids are the primary source of TAG in foxtail millet during chilling response. By contrast, the expression of the sorghum ortholog of *LPP2* was not correlated with TAG abundance, suggesting species-specific differences in membrane lipid funneling to TAG between these two species during chilling stress. *NPC1* expression (**Figure 4**) and PE levels are another example of an unexpected lipase influencing lipid levels. *NPC1* expression was correlated with PE accumulation in foxtail millet and sorghum. *NPC1* produces DAG either through the hydrolysis of PC or MGDG and DGDG, which can in turn be converted to PE (Cao et al. 2016; Krčková et al. 2015). The role of *NPC1* in response to heat stress is known (Krčková et al. 2015). Here, we propose a role for *NPC1* in PE accumulation and chilling tolerance in panicoid grasses.

Overall, we show that despite the conservation of many transcriptional and metabolic responses to chilling stress across species, the unique combination of species employed in our study

allowed us to identify a smaller set of genes more likely to be functionally linked to variation in chilling tolerance than merely due to genetic relatedness. This study provides a framework to probe potential genes whose function in changes to lipid content and composition may not be previously known. For the first time, we also report diel rhythmicity in lipid abundance, saturation, and expression of lipid-related genes in these panicoid grasses during chilling stress.

Supplementary Data:

Figure S1. Minor lipid responses to chilling include effects related to genetic distance and chilling tolerance.

Figure S2. Circos plot showing differential expression of sorghum - foxtail millet orthologous genes.

Figure S3: Venn diagram showing overlap of rhythmic genes under control and chilling stress in sorghum (SB)and foxtail millet (FM).

Figure S4: Total lipid unsaturation in the initial period of chilling stress in foxtail millet, sorghum, and Urochloa**.**

Table S1. Averages and standard errors of each lipid abundance measurements across different time points in foxtail millet, Urochloa, and sorghum.

Table S2. LimoRhyde test of rhythmicity of measured lipids in three grasses.

Table S3. CircaCompare test of rhythmicity for DGDG, PC, and MGDG in three grasses**.** Mesor is average expression, amplitude is the difference between mesor and peak level, phase is when the peak occurs (in radians), and peak time is hours of peak expression after time 0.

Table S4. Averages and standard errors of each lipid unsaturation across different time points in foxtail millet, urochloa, and sorghum.

Table S5. FPKM values of 9778 syntenic gene pairs in sorghum and foxtail millet across each time points with triplicates in chilling stress and control.

Table S6. Differentially regulated orthologs (DROs) between sorghum and foxtail millet using a

680 linear mixed model.

681 **Table S7.** Sorghum and foxtail millet genes classified into 16 clusters based on the ratios of
682 expression values between control and treatments.

683 **Table S8.** Differentially regulated orthologs in sorghum and foxtail millet using conventional
684 clustering method.

685 **Table S9.** High Confidence DROs identified from the overlap of DROs from conventional
686 clustering method and the linear mixed model.

687 **Table S10**. Gene ontology (GO) analysis of 1,708 high-confidence Differentially Regulated
688 Orthologs

689 **Table S11.** Gene expression profiles of sorghum-foxtail millet orthologous genes corresponding
690 to Arabidopsis lipid-related genes.

691 **Table S12.** Log_2 fold change of differentially regulated orthologs in chilling treated sorghum and
692 foxtail millet derived from the list of 356 lipid gene pairs in table S9.

693 **Table S13.** Pearson correlations of foxtail millet and sorghum genes with changes in buildup of
694 each lipid species during chilling stress response.

695 **Table S14.** Pearson correlations of foxtail millet and sorghum genes with changes in breakdown
696 of each lipid species during chilling stress response.

697 **Table S15.** Averages and standard errors of lipid accumulation and unsaturation in Arabidopsis.

698 **Table S16.** CircaCompare test of rhythmicity for DGDG, PC, and MGDG in Arabidopsis. Mesor
699 is average expression, amplitude is the difference between mesor and peak level, phase is
700 when the peak occurs (in radians), and peak time is hours of peak expression after time 0

701 **Table S17.** Averages and standard errors of each lipid accumulation and unsaturation across
702 different time points in control and chilling treated Arabidopsis.

703

704 **Acknowledgments:** We thank Samantha Link and Kandy Hanthorn for their assistance in plant
705 growth and management.

Author Contribution: RLR, JCS, and YZ designed the research; YZ, SM, and DWN performed stress experiments; YZ and DWN processed RNA; SM processed lipids; YZ and SM performed initial data analysis; SKR, YZ, RR, FGH, YQ, and DWN performed final data analyses; SKR, RR, FMH, JCS, and YZ wrote and edited the manuscript.

Conflict of Interest Statement: JCS has equity interests in Data2Bio, LLC; Dryland Genetics Co; and EnGeniousAg LLC. He is a member of the scientific advisory board of GeneSeek. We have no other conflicts to disclose.

Funding Statement: This work was supported by the National Institute of Food and Agriculture at the United States Department of Agriculture grant 2016-67013-24613 to JCS and RLR, the National Science Foundation grants IOS-1845175 to RLR; OIA-1557417 to JCS, and the United States Department of Agriculture Agricultural Research Service award 2030-21000-049-00D to FGH. The project also received support from the United States Department of Agriculture Formula Funds Multistate Hatch Project NEB-30-131.

Data Availability: Sequencing data are available through the NCBI (http://www.ncbi.nlm.nih.gov/bioproject) under accession number SRA: SRP090583 and BioProject: PRJNA344653.

References

Arisz SA, Heo JY, Koevoets IT, Zhao T, van Egmond P, Meyer AJ, Zeng W, Niu X, Wang B, Mitchell-Olds T, Schranz ME, Testerink C. 2018. DIACYLGLYCEROL ACYLTRANSFERASE1 Contributes to Freezing Tolerance. Plant Physiol **177**, 1410-1424.

Barnes AC, Elowsky CG, Roston RL. 2019. An Arabidopsis protoplast isolation method reduces cytosolic acidification and activation of the chloroplast stress sensor SENSITIVE TO FREEZING 2. Plant Signaling & Behavior, 1-7.

Barnes AC, Myers JL, Surber SM, Liang ZK, Mower JP, Schnable JC, Roston RL. 2023. Oligogalactolipid production during cold challenge is conserved in early diverging lineages. Journal of Experimental Botany **74**, 5405-5417.

Benjamini Y, Hochberg Y. 1995. Controlling the False Discovery Rate - a Practical and Powerful Approach to Multiple Testing. Journal of the Royal Statistical Society Series B-Statistical Methodology **57**, 289-300.

Bennetzen JL, Schmutz J, Wang H, Percifield R, Hawkins J, Pontaroli AC, Estep M, Feng L, Vaughn JN, Grimwood J, Jenkins J, Barry K, Lindquist E, Hellsten U, Deshpande S, Wang X, Wu X, Mitros T, Triplett J, Yang X, Ye CY, Mauro-Herrera M, Wang L, Li P, Sharma M, Sharma R, Ronald PC, Panaud O, Kellogg EA, Brutnell TP, Doust AN, Tuskan GA, Rokhsar D, Devos KM. 2012. Reference genome sequence of the model plant Setaria. Nat Biotechnol **30**, 555-561.

Brendel V, Kurtz S, Walbot V. 2002. Comparative genomics of Arabidopsis and maize: prospects and limitations. Genome Biology **3**, REVIEWS1005.

Brozynska M, Furtado A, Henry RJ. 2016. Genomics of crop wild relatives: expanding the gene pool for crop improvement. Plant Biotechnol J **14**, 1070-1085.

Burow G, Burke JJ, Xin ZG, Franks CD. 2011. Genetic dissection of early-season cold tolerance in sorghum (Sorghum bicolor (L.) Moench). Molecular Breeding **28**, 391-402.

Cao H, Zhuo L, Su Y, Sun L, Wang X. 2016. Non-specific phospholipase C1 affects silicon distribution and mechanical strength in stem nodes of rice. Plant J **86**, 308-321.

Chen L, Hu W, Mishra N, Wei J, Lu H, Hou Y, Qiu X, Yu S, Wang C, Zhang H, Cai Y, Sun C, Shen G. 2020. AKR2A interacts with KCS1 to improve VLCFAs contents and chilling tolerance of Arabidopsis thaliana. Plant J **103**, 1575-1589.

Doggett H, Majisu BN. 1968. Disruptive Selection in Crop Development. Heredity **23**, 1-&.

Dohleman FG, Long SP. 2009. More Productive Than Maize in the Midwest: How Does Miscanthus Do It? Plant Physiology **150**, 2104-2115.

Du ZY, Benning C. 2016. Triacylglycerol Accumulation in Photosynthetic Cells in Plants and Algae. Subcell Biochem **86**, 179-205.

Ekman A, Bulow L, Stymne S. 2007. Elevated atmospheric CO2 concentration and diurnal cycle induce changes in lipid composition in Arabidopsis thaliana. New Phytologist **174**, 591-599.

"Finding Groups in Data": Cluster Analysis Extended Rousseeuw et al. [R package cluster version 2.1.4] (2022) (April 3, 2023).

fpc: Flexible Procedures for Clustering. *Comprehensive R Archive Network (CRAN)* (April 3, 2023).

Gentleman RC, Carey VJ, Bates DM, Bolstad B, Dettling M, Dudoit S, Ellis B, Gautier L, Ge YC, Gentry J, Hornik K, Hothorn T, Huber W, Iacus S, Irizarry R, Leisch F, Li C, Maechler M, Rossini AJ, Sawitzki G, Smith C, Smyth G, Tierney L, Yang JYH, Zhang JH. 2004. Bioconductor: open software development for computational biology and bioinformatics. Genome Biology **5**.

Gu Y, He L, Zhao C, Wang F, Yan B, Gao Y, Li Z, Yang K, Xu J. 2017. Biochemical and Transcriptional Regulation of Membrane Lipid Metabolism in Maize Leaves under Low Temperature. Front Plant Sci **8**, 2053.

Hope HJ, Mcelroy A. 1990. Low-Temperature Tolerance of Switchgrass (Panicum-Virgatum L). Canadian Journal of Plant Science **70**, 1091-1096.

Hugly S, Somerville C. 1992. A Role for Membrane Lipid Polyunsaturation in Chloroplast Biogenesis at Low-Temperature. Plant Physiology **99**, 197-202.

Hurry V, Druart N, Cavaco A, Gardeström P, Strand A. 2002. Photosynthesis at low temperatures: A case study with. Plant Cold Hardiness: Gene Regulation and Genetic Engineering, 161-179.

Kaplan F, Guy CL. 2004. β-amylase induction and the protective role of maltose during temperature shock. Plant Physiology **135**, 1674-1684.

Kenchanmane Raju SK, Barnes AC, Schnable JC, Roston RL. 2018. Low-temperature tolerance in land plants: Are transcript and membrane responses conserved? Plant Sci **276**, 73-86.

Kim SC, Edgeworth KN, Nusinow DA, Wang XM. 2023. Circadian clock factors regulate the first condensation reaction of fatty acid synthesis in Arabidopsis. Cell Reports **42**.

Klinska-Bachor S, Kedzierska S, Demski K, Banas A. 2023. Phospholipid:diacylglycerol acyltransferase1-overexpression stimulates lipid turnover, oil production and fitness in cold-grown plants. BMC Plant Biol **23**, 370.

Krckova Z, Brouzdova J, Danek M, Kocourkova D, Rainteau D, Ruelland E, Valentova O, Pejchar P, Martinec J. 2015. Arabidopsis non-specific phospholipase C1: characterization and its involvement in response to heat stress. Front Plant Sci **6**, 928.

Lai X, Bendix C, Yan L, Zhang Y, Schnable JC, Harmon FG. 2020. Interspecific analysis of diurnal gene regulation in panicoid grasses identifies known and novel regulatory motifs. BMC Genomics **21**, 428.

Larcher W. 1995. Photosynthesis as a Tool for Indicating Temperature Stress Events. In: Schulze E-D, Caldwell MM, eds. *Ecophysiology of Photosynthesis*. Berlin, Heidelberg: Springer Berlin Heidelberg, 261-277.

Larran AS, Pajoro A, Qüesta J. 2023. Is winter coming? Impact of the changing climate on plant responses to cold temperature. Plant Cell and Environment **46**, 3175-3193.

Lu HY, Zhang JP, Liu KB, Wu NQ, Li YM, Zhou KS, Ye ML, Zhang TY, Zhang HJ, Yang XY, Shen LC, Xu DK, Li Q. 2009. Earliest domestication of common millet (*Panicum miliaceum*) in East Asia extended to 10,000 years ago. Proceedings of the National Academy of Sciences of the United States of America **106**, 7367-7372.

Lu J, Xu Y, Wang J, Singer SD, Chen G. 2020. The Role of Triacylglycerol in Plant Stress Response. Plants (Basel) **9**.

Lyons JM. 1973. Chilling Injury in Plants. Annual Review of Plant Physiology and Plant Molecular Biology **24**, 445-466.

Maatta S, Scheu B, Roth MR, Tamura P, Li MY, Williams TD, Wang XM, Welti R. 2012. Levels of

leaf phosphatidic acids, phosphatidylserines, and most trienoate-containing polar lipid molecular species increase during the dark period of the diurnal cycle. Frontiers in Plant Science **3**.

Mahboub S, Shomo ZD, Regester RM, Albusharif M, Roston RL. 2021. Three Methods to Extract Membrane Glycerolipids: Comparing Sensitivity to Lipase Degradation and Yield. Methods in molecular biology **2295**, 15-27.

Meng X, Liang Z, Dai X, Zhang Y, Mahboub S, Ngu DW, Roston RL, Schnable JC. 2021. Predicting transcriptional responses to cold stress across plant species. Proceedings of the National Academy of Sciences **118**, e2026330118.

Miquel M, James D, Dooner H, Browse J. 1993. Arabidopsis Requires Polyunsaturated Lipids for Low-Temperature Survival. Proceedings of the National Academy of Sciences of the United States of America **90**, 6208-6212.

Moellering ER, Muthan B, Benning C. 2010. Freezing tolerance in plants requires lipid remodeling at the outer chloroplast membrane. Science **330**, 226-228.

Nakamura Y, Andres F, Kanehara K, Liu YC, Doermann P, Coupland G. 2014. Arabidopsis florigen FT binds to diurnally oscillating phospholipids that accelerate flowering. Nature Communications **5**.

Nishida I, Murata N. 1996. Chilling sensitivity in plants and cyanobacteria: the crucial contribution of memrbane lipids. Ann.Rev.Plant Physiol. **47**, 568.

Panter PE, Muranaka T, Cuitun-Coronado D, Graham CA, Yochikawa A, Kudoh H, Dodd AN. 2019. Circadian Regulation of the Plant Transcriptome Under Natural Conditions. Frontiers in Genetics **10**, 1239.

Pardo J, VanBuren R. 2021. Evolutionary innovations driving abiotic stress tolerance in C grasses and cereals. Plant Cell **33**, 3391-3401.

Parsons R, Parsons R, Garner N, Oster H, Rawashdeh O. 2020. CircaCompare: a method to estimate and statistically support differences in mesor, amplitude and phase, between circadian rhythms. Bioinformatics **36**, 1208-1212.

Pessoa M, Martins AM, Ferreira ME. 2017. Molecular dating of phylogenetic divergence between
species based on complete chloroplast genomes. BMC Genomics **18**.

Quinn PJ, Joo F, Vigh L. 1989. The role of unsaturated lipids in membrane structure and stability. Prog Biophys Mol Biol **53**, 71-103.

Ray DK, Mueller ND, West PC, Foley JA. 2013. Yield Trends Are Insufficient to Double Global Crop Production by 2050. PloS one **8**, e66428.

Sandve SR, Rudi H, Asp T, Rognli OA. 2008. Tracking the evolution of a cold stress associated gene family in cold tolerant grasses. BMC Evolutionary Biology **8**.

Schnable J, Zang Y, W. C. Ngu D. 2016. Pan-Grass Syntenic Gene Set (sorghum referenced). figshare.

Singer JM, Hughey JJ. 2019. LimoRhyde: A Flexible Approach for Differential Analysis of Rhythmic Transcriptome Data. J Biol Rhythms **34**, 5-18.

Taylor AO, Rowley JA. 1971. Plants under Climatic Stress .1. Low Temperature, High Light Effects on Photosynthesis. Plant Physiology **47**, 713-&.

Trapnell C, Williams BA, Pertea G, Mortazavi A, Kwan G, van Baren MJ, Salzberg SL, Wold BJ, Pachter L. 2010. Transcript assembly and quantification by RNA-Seq reveals unannotated transcripts and isoform switching during cell differentiation. Nat Biotechnol **28**, 511-515.

Uemura M, Joseph RA, Steponkus PL. 1995. Cold Acclimation of Arabidopsis thaliana (Effect on Plasma Membrane Lipid Composition and Freeze-Induced Lesions). Plant Physiol **109**, 15-30.

Wang Z, Benning C. 2011. Arabidopsis thaliana polar glycerolipid profiling by thin layer chromatography (TLC) coupled with gas-liquid chromatography (GLC). J Vis Exp.

Wu TD, Reeder J, Lawrence M, Becker G, Brauer MJ. 2016. GMAP and GSNAP for Genomic Sequence Alignment: Enhancements to Speed, Accuracy, and Functionality. Methods in molecular biology **1418**, 283-334.

Xu C, Shanklin J. 2016. Triacylglycerol Metabolism, Function, and Accumulation in Plant Vegetative Tissues. Annual Review of Plant Biology, Vol 62 **67**, 179-206.

Yan L, Kenchanmane Raju SK, Lai X, Zhang Y, Dai X, Rodriguez O, Mahboub S, Roston RL, Schnable JC. 2019. Parallels between natural selection in the cold-adapted crop-wild relative Tripsacum dactyloides and artificial selection in temperate adapted maize. The Plant Journal **0**.

Yang X, Wan Z, Perry L, Lu H, Wang Q, Zhao C, Li J, Xie F, Yu J, Cui T, Wang T, Li M, Ge Q. 2012. Early millet use in northern China. Proc Natl Acad Sci U S A **109**, 3726-3730.

Zhang G, Liu X, Quan Z, Cheng S, Xu X, Pan S, Xie M, Zeng P, Yue Z, Wang W, Tao Y, Bian C, Han C, Xia Q, Peng X, Cao R, Yang X, Zhan D, Hu J, Zhang Y, Li H, Li H, Li N, Wang J, Wang C, Wang R, Guo T, Cai Y, Liu C, Xiang H, Shi Q, Huang P, Chen Q, Li Y,

Wang J, Zhao Z, Wang J. 2012. Genome sequence of foxtail millet (Setaria italica) provides insights into grass evolution and biofuel potential. Nat Biotechnol **30**, 549-554.

Zhang Y, Ngu DW, Carvalho D, Liang Z, Qiu Y, Roston RL, Schnable JC. 2017. Differentially Regulated Orthologs in Sorghum and the Subgenomes of Maize. Plant Cell **29**, 1938-1951.

Zoldan D, Band RS, Guy CL, Porat R. 2012. Understanding Chilling Tolerance Traits Using Arabidopsis Chilling-Sensitive Mutants. In: Ahmad P, Prasad MNV, eds. *Environmental Adaptations and Stress Tolerance of Plants in the Era of Climate Change*. New York, NY: Springer New York, 159-173.

Figure Legends

Figure 1 Foxtail millet is a chilling-tolerant representative of the panicoid grass clade. **(A)** Evolutionary relationships of the four species evaluated with rice as an outgroup. Numbers indicate divergence time as reported in Zhang et al. and Pessoa-Filho et al. (23, 58) **(B)** Normalized relative CO_2 assimilation rates for panicoid grass species with differing degrees of sensitivity or tolerance to chilling stress. CO_2 assimilation was measured after treatment at 6°C for indicated times below (1 day or 8 days) followed by an overnight return to 30°C of approximately 10 hours. Leaf area was measured immediately after assimilation. Individual data points are jittered on the x-axis to avoid overlap. Lines indicate mean values for each species across three replicates and whiskers represent standard error of the mean. **(C)** Phenotypic response of foxtail millet, Urochloa, and sorghum to 6°C chilling stress for 14 days, followed by 2 days of return to 30°C. Scale bars, 6cm.

Figure 2. Lipid responses to chilling include effects related to genetic distance and chilling tolerance.

The relative abundance of specific lipid species exhibits multiple sequential changes in the first 24 hours of exposure to chilling stress. In all panels, the x-axis indicates the time in hours (h) **(A)** Mole percent abundance of lipids relative to all fatty acid-containing lipids for the following lipid classes: monogalactosyldiacylglycerol (MGDG), digalactosyldiacylglcyerol (DGDG), and phosphatidylcholine (PC) in foxtail millet, Urochloa, and sorghum. **(B)** Unsaturation index, calculated as the average number of double bonds per fatty acid for all fatty acid-containing lipids: MGDG, DGDG, and PC.P-values were determined using Fisher's least significant difference (LSD). '*' denotes p-value < 0.05, '**' p-value < 0.01, and '***' p-value < 0.001. **(C)** Structural models of major lipids MGDG, DGDG, and PC, where blue indicates the hydrophilic

head group and orange indicates the hydrophobic tail group. **(D)** Total unsaturation index, calculated as the average number of double bonds per fatty acid for all fatty acid-containing lipids. For all samples, n was between 3 and 8 biological replicates.

Figure 3. Syntenic orthologs in sorghum and foxtail millet show differential regulation during chilling stress.

Heatmap representation of log2 fold change values for chilling stressed samples compared to control in sorghum and foxtail millet at different time points. Lipid related gene pairs that overlapped with high-confidence differentially regulated orthologs were considered and classified into lipid biosynthesis, lipid metabolism, and phospholipid signaling. Genes names in the center are suggestive only and derived from best-hit Arabidopsis genes.

Figure 4. Correlation of lipid and transcript abundances in the glycerolipid biosynthesis pathway allows identification of candidate genes.

(A) Diagram of the glycerolipid biosynthesis pathway with lipid species shown in bold font and the enzymes responsible for each step denoted next to the corresponding arrows. **(B, C)** Heatmaps showing transcript abundance for candidate genes in lipid metabolism and abundance of lipid species (in bold font) at different time points for DGDG **(B)** and phosphatidylethanolamine (PE) **(C)**. Significant correlations measured by pearson correlation, between lipid changes and transcript abundance in either sorghum or foxtail millet are indicated by '*' after the gene name.

Figure 5. Time-series profiles of Arabidopsis lipid abundance and unsaturation during chilling or control conditions.

(A) Mole percent abundance of lipids relative to all fatty acid-containing lipids for the following

lipid classes: monogalactosyldiacylglycerol (MGDG), digalactosyldiacylglcyerol (DGDG), and phosphatidylcholine (PC) in Arabidopiss during chilling or control conditions. **(B)** Unsaturation index, calculated as the average number of double bonds per fatty acid for MGDG, DGDG, and PC. **(C)** Unsaturation index, calculated as the average number of double bonds per fatty acid for all fatty acid-containing lipids. Significant p-values determined using Fisher's least significant differences. *' denotes p-value < 0.05, '**' p-value < 0.01, and '***' p-value < 0.001 **(D)** Diagram showing daily and seasonal fluctuation of temperature during the plants' growth cycle. For all samples, n was between 3 and 8 biological replicates.

Figure 6. Comparison of rhythmicity and differential rhythmicity in sorghum and foxtail millet lipid related genes.

(A) Venn diagram showing the extent of overlap between rhythmic genes in sorghum and/or foxtail millet identified by *LimoRhyde* analysis under control conditions (244 genes in the green circle) and sorghum differentially rhythmic (DR) under control conditions compared to chilling treatment (101 genes in the pink circle) and foxtail millet DR under control conditions compared to chilling treatment (142 genes in the purple circle). The union of these three data sets is 36 genes representing rhythmic genes under control conditions that change their rhythmicity in response to chilling temperature in both foxtail millet and sorghum. **(B, C)** An example of a rhythmic gene *DGD1* showing a similar diel expression pattern under control conditions and changed rhythmicity during chilling stress response in sorghum **(B)** and foxtail millet **(C)**. *DGD1* expression is shown as average FPKM values from three biological replicates and the standard error of mean.

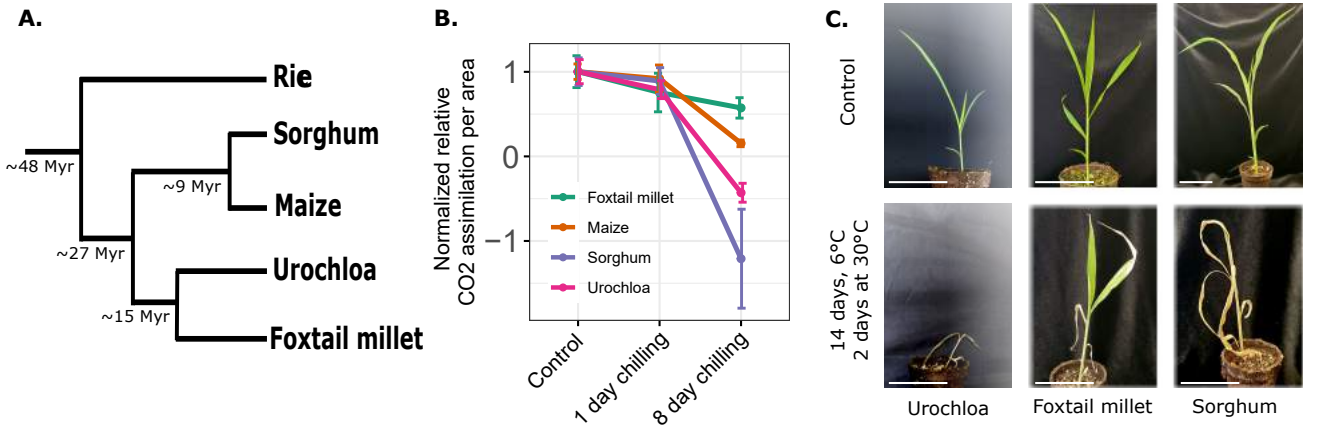

Figure 1: Foxtail millet is a chilling-tolerant representative of the panicoid grass clade. A) Evolutionary relationship of the four species evaluated with rice as an outgroup. Numbers indicate divergence time as reported in Zhang et al. 2017 and Pessoa-Filho et al. 2017 (B) Normalized relative CO_2 assimilation rates for panicoid grass species with differing degrees of sensitivity or tolerance to chilling stress. CO_2 assimilation was measured after treatment at 6°C for indicated times (1 day or 8 days) followed by return to 30°C for approximately 10 hours. Leaf area was measured immediately after assimilation. Individual data points are jittered on the x-axis to avoid overlap. Lines indicate mean values for each species across three replicates and whiskers represent standard error of the mean. (C) Phenotypic response of Urochloa, foxtail millet, and sorghum to 6°C chilling stress for 14 days, followed by 2 days of return to 30°C. Scale bars, 6cm.

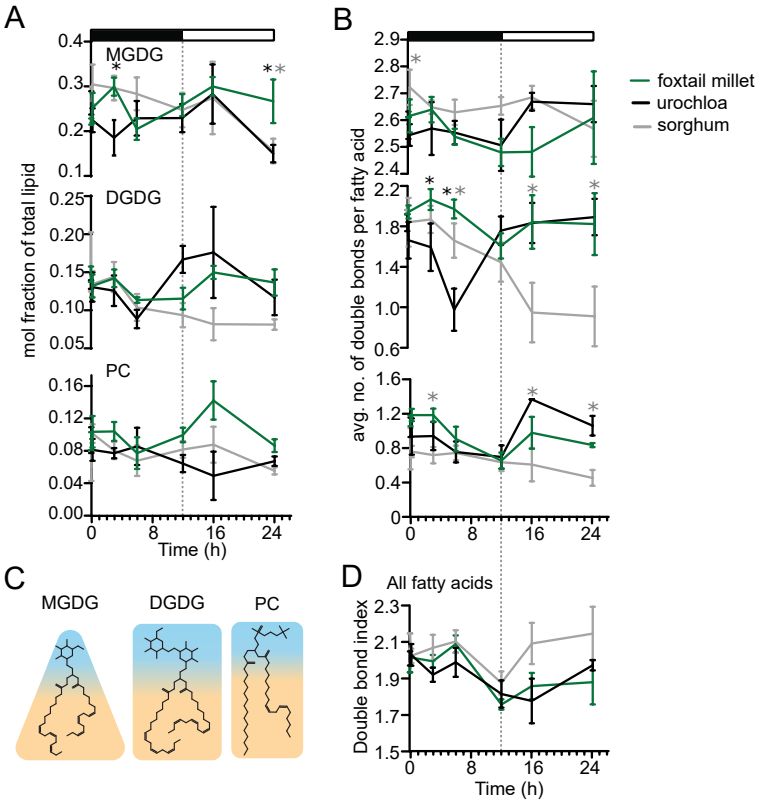

Figure 2. Lipid responses to chilling include effects related to genetic distance and chilling tolerance. The relative abundance of specific lipid species exhibits multiple sequential changes in the first 24 hours of exposure to chilling stress. In all panels, the x-axis indicates the time in hours (h). (A) Mole percent abundance of lipids relative to all fatty acid-containing lipids for the following lipid classes: monogalactosyldiacylglycerol (MGDG), digalactosyldiacylglcyerol (DGDG), and phosphatidylcholine (PC) in foxtail millet, Urochloa, and sorghum. (B) Unsaturation index, calculated as the average number of double bonds per fatty acid for all fatty acid-containing lipids: MGDG, DGDG, and PC.P-values were determined using Fisher's least significant difference (LSD). '*' denotes p-value < 0.05, '**' p-value < 0.01, and '***' p-value < 0.001. (C) Structural models of major lipids MGDG, DGDG, and PC. (D) Total unsaturation index, calculated as the average number of double bonds per fatty acid for all fatty acid-containing lipids. For all samples, n was between 3 and 8 biological replicates.

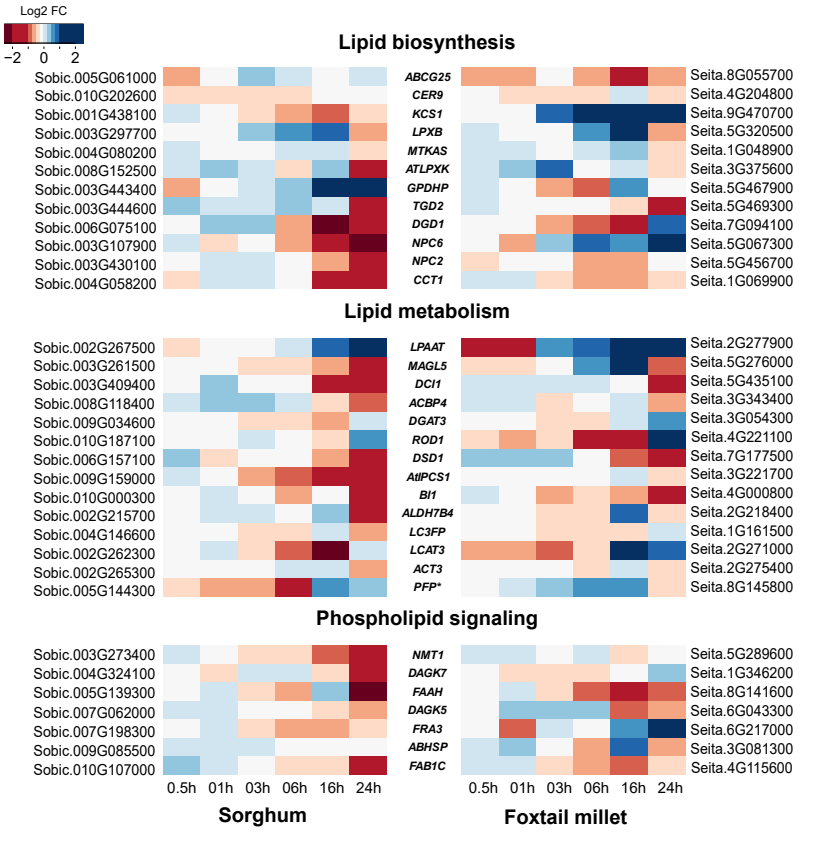

Figure 3. Syntenic orthologs in sorghum and foxtail millet show differential regulation during chilling stress. Heatmap representation of log2 fold change values for chilling stressed samples compared to control in sorghum and foxtail millet at different time points. Lipid related gene pairs that overlapped with high-confidence differentially regulated orthologs were considered and classified into lipid biosynthesis, lipid metabolism, and phospholipid signaling. Genes names in the center are suggestive only and derived from best-hit Arabidopsis genes.

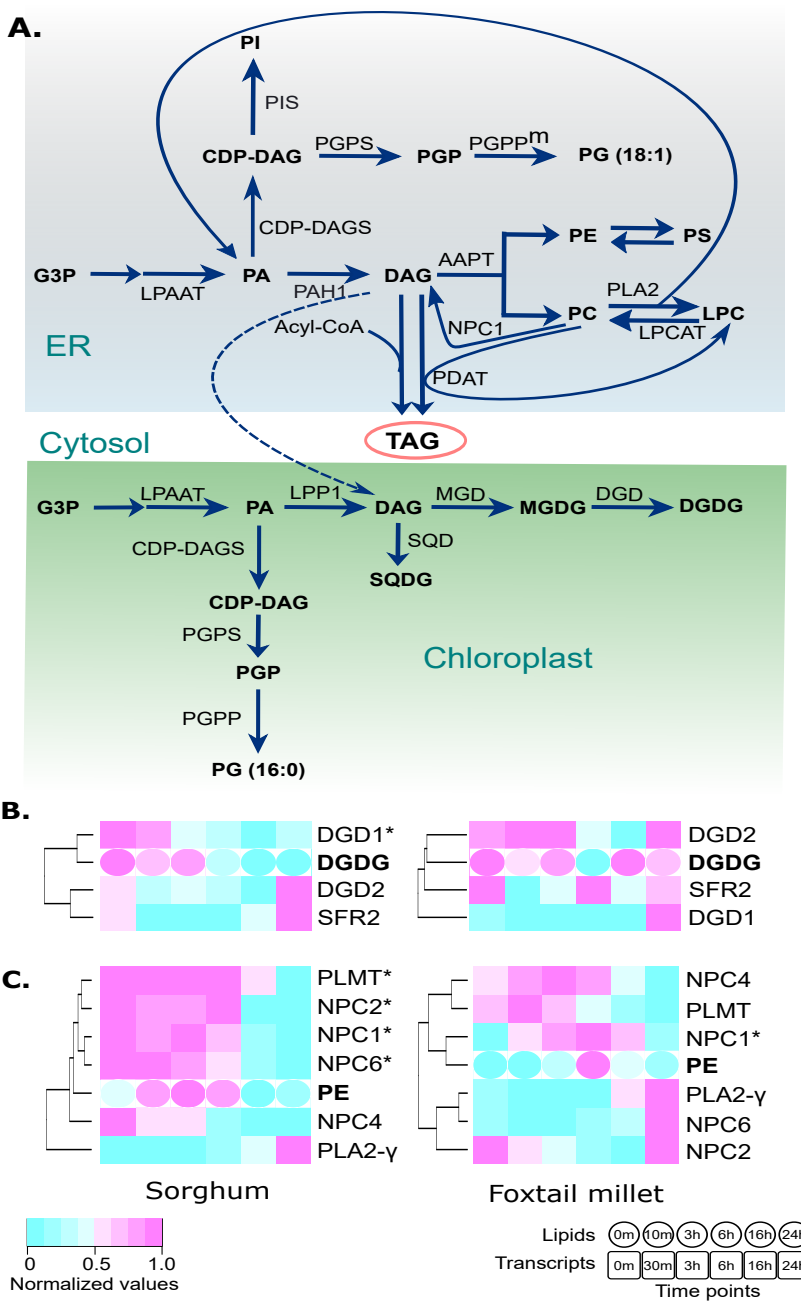

Figure 4. Correlation of lipid and transcript abundances in the glycerolipid biosynthesis pathway allows identification of candidate genes. (A) Diagram of the glycerolipid biosynthesis pathway with lipid species shown in bold font and the enzymes responsible for each step denoted next to the corresponding arrows. (B, C) Heatmaps showing normalized transcript abundance for candidate lipid-related genes and normalized lipid abundance (in bold font) at different time points (12 h timepoint for lipid is removed because of lack of corresponding transcript data) for DGDG (B) and phosphatidylethanolamine (PE) (C). Significant correlations measured by pearson correlation, between lipid changes and transcript abundance in either sorghum or foxtail millet are indicated by '*' after the gene name.

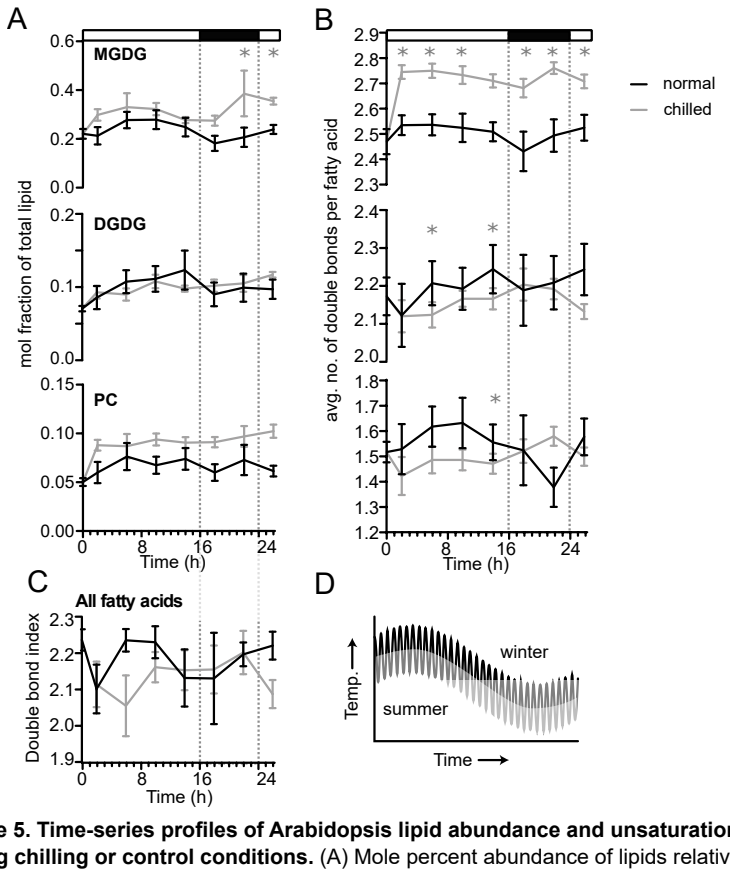

Figure 5. Time-series profiles of Arabidopsis lipid abundance and unsaturation during chilling or control conditions. (A) Mole percent abundance of lipids relative to all fatty acid-containing lipids for the following lipid classes: monogalactosyldiacylglycerol (MGDG), digalactosyldiacylglcyerol (DGDG), and phosphatidylcholine (PC) in Arabidopiss during chilling or control conditions. (B) Unsaturation index, calculated as the average number of double bonds per fatty acid for MGDG, DGDG, and PC. (C) Unsaturation index, calculated as the average number of double bonds per fatty acid for all fatty acid-containing lipids. Significant p-values determined using Fisher's least significant differences. '*' denotes p-value < 0.05, '**' p-value < 0.01, and '***' p-value < 0.001 (D) Diagram showing daily and seasonal fluctuation of temperature during the plants growth cycle.

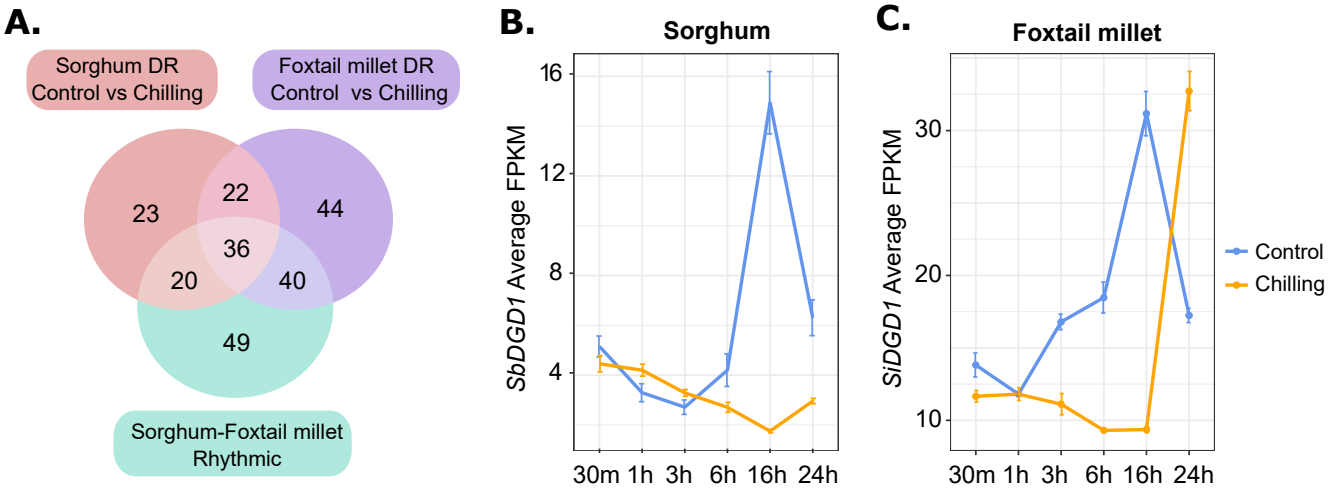

Figure 6 Comparison of rhythmicity and differential rhythmicity in sorghum and foxtail millet lipid related genes. (A) Venn diagram showing the extent of overlap between rhythmic genes in sorghum and/or foxtail millet identified by LimoRhyde analysis under control conditions (244 genes in the green circle) and sorghum differentially rhythmic (DR) under control conditions compared to chilling treatment (101 genes in the pink circle) and foxtail millet DR under control conditions compared to chilling treatment (142 genes in the purple circle). The union of these three data sets is 58 genes representing rhythmic genes that change their rhythmicity in response to chilling temperature in both foxtail millet and sorghum. (B,C) An example of a rhythmic gene DGD1 showing a similar diel expression pattern under control conditions and changed rhythmicity during chilling stress response in sorghum (B) and foxtail millet (C). DGD1 expression is shown as average FPKM values from three biological replicates and the standard error of mean.